Dalton Transactions

PAPER

View Article Online
View Journal | View Issue

Cite this: *Dalton Trans.*, 2014, **43**, 12689

Pyrophosphate selective fluorescent chemosensors: cascade recognition of nuclear stain mimicking DAPI†

Shyamaprosad Goswami,*[a] Avijit Kumar Das,[a] Bholanath Pakhira,[a] Sohini Basu Roy,[a] Anup Kumar Maity,[b] Partha Saha[b] and Sabyasachi Sarkar[a]

Received 29th April 2014,
Accepted 23rd June 2014

DOI: 10.1039/c4dt01262c

www.rsc.org/dalton

A new zinc(II) complex with a condensed hydroxynaphthyl pyridine (SPHN) as the coordinated ligand has been synthesized for the selective recognition of pyrophosphate (PPi) over other anions including phosphate in a mixed aqueous solution. The fluorescence enhancement of SPHN in association with Zn^{2+} ions is quenched in the presence of intracellular pyrophosphate. This phenomenon is utilized in the construction of a logic gate. The binding of SPHN with Zn^{2+} and its displacement by PPi have been established by photophysical investigation and supported by the DFT level of studies. The development of blue fluorescence in the {**SPNH–Zn**} complex upon binding of zinc with **SPHN** is shown to be useful as a nucleus marker in a cell similar to the commercially available staining compound, DAPI (diamino-2-phenylindole).

Combinatorial chemistry is widely used for substrate preference and in understanding the mechanistic pathways of various enzymatic reactions in chemical biology, medical and pharmaceutical sciences or in diagnostic studies in relevance to drug interactions.[1] However, the use of fluorescent dyes in such applications is still in its infancy.[2] The most common strategy used for this is linking of the fluorescent dye molecule through an appropriate conduit for signal transduction to a designed receptor fragment which is known to have high specificity towards the desired analyte. The receptor-analyte binding is expected to influence the luminescence behavior of the dye moiety. In this regard, the "turn-on and turn-off"-type sensor has a distinct edge over others due to the unambiguous assignment in detection processes.[3] The development of molecular-recognition and sensing systems for anions and cations has received considerable attention in recent years.[4]

Phosphates are among the most important anions in biological systems, as they play significant roles in many biological processes, such as cellular ATP hydrolysis and DNA and RNA polymerization reactions,[5] and are part of nucleosides and nucleotides.[6] Recently, the detection of PPi has become an important issue for cancer research[7] and for rheumatological disorder that arises due to the accumulation of crystals of calcium pyrophosphate dihydrate in the connective tissues. Thus, the specific recognition and sensing of PPi under physiological conditions is of immense significance.[8] However, due to the high solvation energy in water (584 kcal mol^{-1}) of PPi and the presence of other competitive anions, selective and specific sensing of PPi in aqueous medium based on the H-bonding interaction is very difficult. Recently it has been revealed that certain transition metal complexes are found to be appropriate for use as receptors for the selective recognition of these phosphate ions in an aqueous environment where the cavity formed by the metal ion with the receptor provides a cooperative binding site for the desired phosphate derivative.[9] However, examples of selective sensor molecules for PPi are rather limited in the literature[10] and the potential of such a PPi sensor for bioanalytical application is at the primitive stage.

In this report, we show that the pyridine–naphthalene based ligand, **SPHN**, when forming a complex with Zn^{2+} is highly fluorescent. This **SPHN–Zn** complex has been utilized as a receptor for PPi in aqueous medium by a metal displacement approach which results in the quenching of fluorescence produced by the complex formed by Zn^{2+} with **SPHN**.

Interestingly the specificity of PPi over related analogues such as ATP and inorganic phosphate (Pi) makes the **SPHN–Zn** complex a selective and specific channel for PPi and such a reactivity is retained even with the biological system. The synthesis of **SPHN** is accomplished as presented in Scheme 1. Condensation of 2,6-pyridine-diamine amine with chloroacetyl chloride in dry dichloromethane produces compound **A**.

[a]*Department of Chemistry, Indian Institute of Engineering Science and Technology, Shibpur, Howrah-711 103, India. E-mail: spgoswamical@yahoo.com; Fax: +91 33 2668 2916; Tel: +91 33 2668 2961-3*

[b]*Crystallography and Molecular Biology Division, Saha Institute of Nuclear Physics, Kolkata 700064, West Bengal, India*

†Electronic supplementary information (ESI) available. See DOI: 10.1039/c4dt01262c

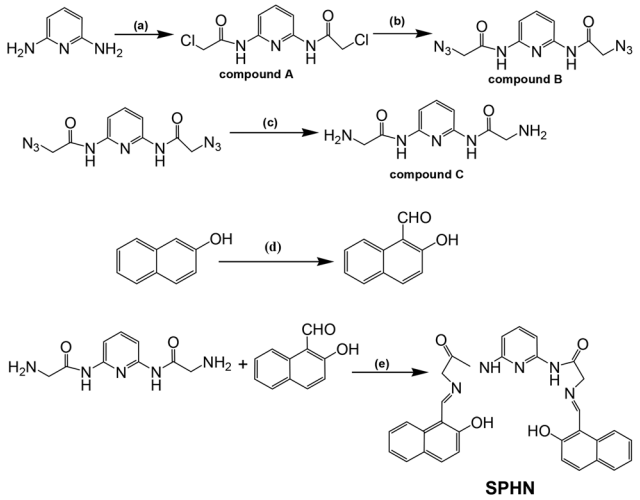

Scheme 1 (a) Chloroacetyl chloride, dry DCM, at 0 °C, 6 h. (b) NaN_3, dry DMF, 60–80 °C, overnight. (c) H_2/Pd-C, in dry MeOH, 4 h. (d) $CHCl_3$, NaOH, EtOH, 6 h. (e) Dry MeOH, rt, 6 h.

The azide compound **B** was then synthesized by the chlorine displacement reaction of compound **A** with sodium azide in dry DMF. The amine compound **C** was then obtained by the hydrogenation of compound **B** in dry methanol. The final compound **SPHN** was obtained by the condensation of compound **C** with 2-hydroxy-1-naphyl aldehydes. **Receptor 1** (the **SPHN–Zn** complex as **SPHN** was found to be a selective sensor for Zn^{2+}) was then synthesized by stirring a methanolic solution of **SPHN** with $ZnCl_2$. **Receptor 1** has been proved to be specific for recognition of PPi as discussed below.

Results and discussion

The **SPHN** ligand has been tested first as a selective sensor for the Zn^{2+} ion. The absorption and fluorescence properties of **SPHN** were tested in a CH_3CN–aqueous HEPES buffer (7/3, v/v, at 25 °C) at pH 7.4.

The UV-vis titration experiment was carried out in CH_3CN–aqueous HEPES buffer at the 2×10^{-5} M concentration of **SPHN** solution upon addition of an incremental amount of zinc chloride ($c = 2 \times 10^{-4}$ M) (Fig. 1). The UV-vis spectrum of

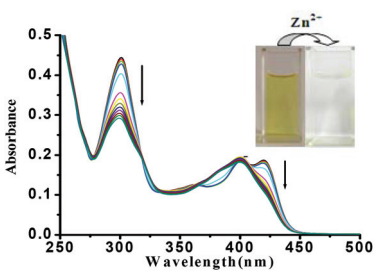

Fig. 1 UV-vis absorption spectra of the receptor **SPHN** ($c = 2 \times 10^{-5}$ M) with zinc chloride ($c = 2 \times 10^{-4}$ M) in CH_3CN–10 mM aqueous HEPES buffer (7/3, v/v, 25 °C) at pH = 7.4.

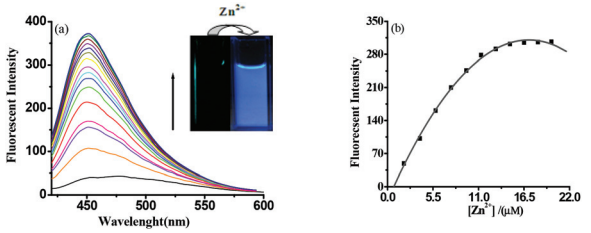

Fig. 2 (a) Fluorescence spectra of the receptor **SPHN** ($c = 2 \times 10^{-5}$ M) with zinc chloride ($c = 2 \times 10^{-4}$ M) in CH_3CN–10 mM aqueous HEPES buffer (7/3, v/v, 25 °C) at pH = 7.4. Right inset: the appearance of blue fluorescence of **SPHN** on addition of Zn^{2+}. (b) Fluorescence intensity of the receptor (2×10^{-5} M) at 450 nm as a function of [Zn^{2+}] (2×10^{-4} M).

the receptor **SPHN** exhibits three absorption bands at 300, 399 and 420 nm. Upon gradual increase of the Zn^{2+} ion concentration the bands at 300 and 420 nm gradually lose their intensity and the yellow color of the receptor solution finally becomes colorless. This is due to the formation of a new complex between the host and the guest (receptor–metal).

To explore the binding affinity of **SPHN** towards different metal ions (Co^{2+}, Hg^{2+}, Mn^{2+}, Ni^{2+}, Pb^{2+}, Cd^{2+}, Zn^{2+}, Mg^{2+}, Cu^{2+}, Fe^{3+}, Cr^{3+}, Ca^{2+}, Mg^{2+}, Na^{+}, K^{+} as their chloride salts), the fluorescence spectral response of **SPHN** was checked in the presence of each of these metal ions in CH_3CN–aqueous HEPES buffer (7/3, v/v, pH = 7.4) solution. However, treatment with an aqueous solution containing Zn^{2+} ions resulted in a large (10 fold) increase in fluorescence intensity at a wavelength of 450 nm on excitation at 400 nm (Fig. 2). Upon complexation with zinc ions, a large CHEF (chelation-enhanced fluorescence) effect was observed which tends to produce a strong 'switch on' blue fluorescence. **SPHN** as a free ligand showed a weak fluorescence at 450 nm on excitation at 400 nm with a low quantum yield $\Phi_0 = 0.044$.

Upon addition of an increasing amount of Zn^{2+} ions, about 21-fold increase in the fluorescence quantum yield (Φ/Φ_0 = 0.940/0.044 = 21, $\lambda_{max\ (em)}$ = 400 nm) (ESI†) was observed. In contrast, upon addition of other relevant 3d metal ions no fluorescence was observed and thus other metal ions remain virtually silent except that the higher congener of the zinc ion, the Cd^{2+} ion, displayed very weak fluorescence (Fig. 3). Zn^{2+}

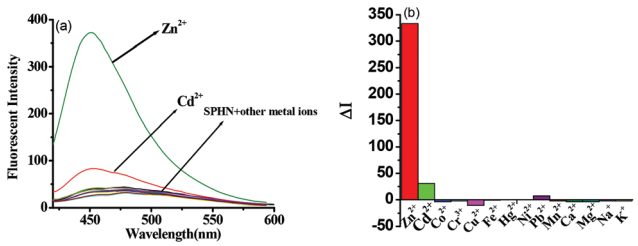

Fig. 3 (a) Fluorescence spectra of the receptor **SPHN** ($c = 2 \times 10^{-5}$ M) upon titration with 4.0 equiv. of each of the different guest cations ($c = 2 \times 10^{-4}$ M) in CH_3CN–10 mM aqueous HEPES buffer (7/3, v/v, 25 °C) at pH 7.4. (b) Change in the emission intensity as bar representation of the sensor after addition of 4.0 equiv. of each of the guest cations to CH_3CN–10 mM aqueous HEPES buffer (7/3, v/v, 25 °C) at 450 nm.

ions induce an increase in the emission intensity of **SPHN** as shown by red bars and the green bar indicates the slight interference by the Cd^{2+} ion (Fig. 3b). The 1 : 2 stoichiometry for the host–guest complexation was confirmed by Job plot analysis (Fig. S1†). This implies that two zinc ions are incorporated into the cavity of **SPHN** by the probable four co-ordination binding pattern of the zinc ion. From the titration following electronic spectroscopy the association constant (K_a) of **SPHN** with Zn^{2+} ions is found to be 1×10^4 M^{-1} (error < 10%)[11] (ESI†).

The sensing ability of **SPHN** towards zinc ions has also been investigated at different pH values which remained significantly high in the physiological pH range as shown in Fig. S7.† The sensor, **SPHN**, had no fluorescence response to Zn^{2+} in the acidic (lower) pH range which may be due to the weak coordination capability of zinc ions[12] possibly by the protonation of the co-ordination sites of the ligand. Satisfactory Zn^{2+} sensing abilities were exhibited when the pH was increased from 6.1 to 13 and it reached the maximum value at pH 7.4 indicating that the **SPHN** possesses high selectivity and sensitivity towards zinc in the physiological pH window (Fig. S8,† red box). To explore the specificity of **SPHN** for Zn^{2+}, experiments were carried out in the presence of Zn^{2+} ions mixed with other competitive metal ions.

As shown in Fig. 4(a), the fluorescence enhancement due to binding with zinc remains unperturbed (shown by brown bars) and the other interfering metal ions remained neutral toward Zn^{2+} ions (shown by blue bars) in CH_3CN–aqueous HEPES buffer (7/3, v/v) solution. To investigate the application of SPHN as a sensor the color changes in test strips were analysed as shown in Fig. 4(b). Test strips were prepared by immersing TLC plate strips in a CH_3CN–aqueous HEPES buffer (7/3, v/v) of **SPHN** ($c = 4.0 \times 10^{-3}$ M) and then drying these strips in air. As shown in Fig. 4(b), with the increase in Zn^{2+} concentration the intensity of the blue color of the test strip optimally increases (downward arrow) and on the addition of PPi to **SPHN–Zn** solution the developed color gradually fades on test strips (upward arrow). Thus in the solid phase, this 'off–on–off' color appearance in the test strips by the alternate use of Zn^{2+} and PPi makes **SPHN** a reversible sensor for these two analytes. The development of such dipsticks is useful as instant qualitative information may be obtained without resorting to the time consuming instrumental analysis.

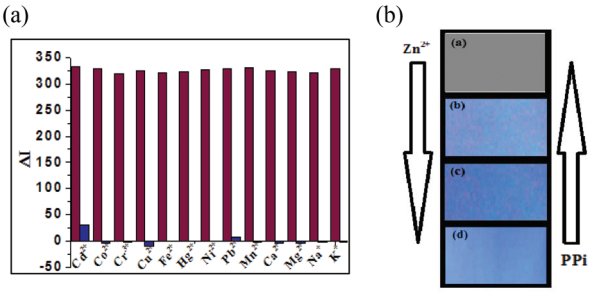

Fig. 4 (a) Metal ion selectivity profile of the sensor **SPHN** (20 μM): (blue bar) change of emission intensity of sensor + 8.0 equiv. of different interfering M^{n+}; (brown bar) change of emission intensity of sensor + 8.0 equiv. M^{n+}, followed by 4.0 equiv. Zn^{2+} at 450 nm. (b) Color changes visualized on TLC plate strips of (a) SPHN (c = 4.0 × 10 M) and during increasing concentrations of Zn^{2+} (lower arrow) and PPi (upper arrow) at concentration (b) 2.0×10^{-5} M, (c) 1.0×10^{-4} M and (d) 1.0×10^{-3} M to the receptor solution in CH_3CN–10 mM aqueous HEPES buffer (7/3, v/v) solution.

The facile and selective formation of the new complex **SPHN–Zn** proves the highest affinity of Zn^{2+} ions towards the pyridine-hydroxynaphthyl fragment of the receptor **SPHN**. The complex was isolated as a pure solid and characterized using standard analytical and spectroscopic techniques. In mass spectrometry, the peak at m/z = 656.0172 [corresponding to $C_{31}H_{21}N_5O_4Zn_2 + H^+]^+$ in HRMS spectra (Fig. S21†) indicates the formation of **Receptor 1** as shown in Scheme 2. The ^{1}H NMR titration curve also supports the formation of such complexation by deprotonation of **SPHN**. The formation of such a complex has also been explained by the density functional theory (DFT). In order to explore the potential bioanalytical application of this synthesized **SPHN–Zn** complex (**Receptor 1**), we have investigated its interaction with common anionic analytes and nucleotides.

Receptor 1 ($c = 2 \times 10^{-5}$ M) in CH_3CN–aqueous HEPES buffer (7/3, v/v) solution at pH = 7.4 was used for recording the emission spectra in the absence and in the presence of the corresponding tetrabutylammonium salts of the common anionic analytes and nucleotides ($c = 2 \times 10^{-4}$ M). A turn-off fluorescence response was observed for the emission band with a maximum at 450 nm in the presence of an externally added solution of PPi (Fig. 5). Interestingly other anions and nucleotides like F^-, AcO^-, Cl^-, Br^-, I^-, $C_6H_5COO^-$, ATP, DHP, NO_3^-, NO_2^-, SO_3^{2-} and HPO_4^{2-} as their tetrabutyl ammonium salts do not react with **Receptor 1** and are thus unable to extrude the zinc ion from the complex as shown in Fig. 6(a). The competition experiment also determined the PPi selectivity of **Receptor 1** in the presence of other competitive interfering anions. As shown in Fig. 6(b), the deep blue fluorescence enhancement by Zn^{2+} ions in **Receptor 1** remains unaffected in the presence of various anions (blue bar) and the deep blue color is significantly quenched by the addition of PPi even in the presence of various interfering anions (green bar). This indicates that **Receptor 1** is highly selective and specific to bind PPi and remained insensitive towards other phosphates as well as other interfering anions.

The binding mode in **SPHN** for zinc ions in the solution phase has been verified using the ^{1}H NMR titration curve (Fig. S7†) which is supported by the density functional theory (DFT). Naphthyl–OH and amide –NH are found to be the binding sites for the co-ordination of zinc ions to **SPHN**. The ^{1}H NMR titration curve showed that after the addition of zinc to the **SPHN** (receptor) solution, the Ha peak at δ 13.75 ppm (of –OH proton intramolecularly six membered hydrogen bonded) and the Hb proton at δ 10.45 ppm (of –NH) disappear. The other aromatic protons remain virtually unperturbed due to the zinc ion co-ordination. Furthermore when PPi is added to the solution of the zinc complex, the two small peaks

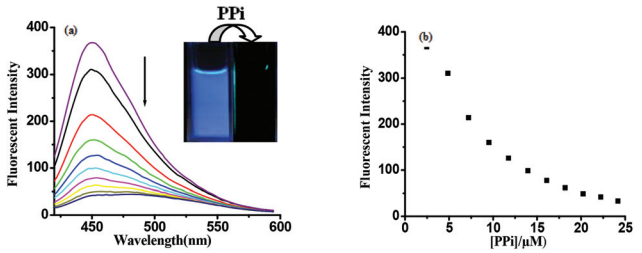

Fig. 5 (a) Fluorescence spectra of **Receptor 1** (c = 2 × 10^{-5} M) in CH_3CN–10 mM aqueous HEPES buffer (7/3, v/v, 25 °C) upon titration with 2.0 equiv. of PPi (2 × 10^{-4} M) at pH 7.4. (b) Fluorescence intensity of the receptor (c = 2 × 10^{-5} M) at 450 nm as a function of [PPi] (c = 2 × 10^{-4} M).

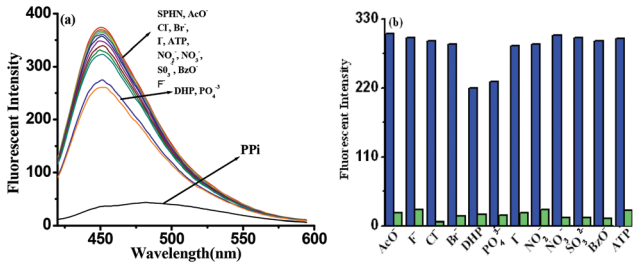

Fig. 6 (a) Change of emission intensity of the sensor after addition of 2.0 equiv. of each of the guest anions to CH_3CN–10 mM aqueous HEPES buffer (7/3, v/v, 25 °C) at pH 7.4. (b) Anion selectivity profile of the sensor **SPHN–Zn** (**Receptor 1**) (20 μM): (blue bar) change of the emission intensity of **Receptor 1** + 5.0 equiv. of different anions; (green bar) change of the emission intensity of **Receptor 1** + 5.0 equiv. of different anions, followed by 2.0 equiv. PPi at 450 nm.

related to Ha for –OH and Hb for –NH appear due to pyrophosphate induced decomplexation (Fig. S7†).

In biological systems PPi is released in the presence of ATP and other phosphates. Therefore the best sensor for detecting PPi in aqueous medium must show specificity and high sensitivity for PPi over ATP and P_i. As shown in Fig. 5(a), the addition of PPi to the solution of **Receptor 1** induces a dramatic fluorescence quenching effect. The other phosphates such as HPO_4^{2-} (P_i) cause negligible reduction in the intensity of fluorescence compared with the intense quenching by PPi. PPi itself does not show any response to **SPHN** in the emission and absorption spectrum (Fig. S5†). But its addition causes drastic quenching of the enhanced fluorescence due to the complex formation of Zn^{2+} with **SPHN**. Interestingly the fluorescence can be restored on fresh addition of Zn^{2+} ions (Fig. S6†). The alternate addition of PPi to quench the fluorescence followed by addition of zinc ions to restore the fluorescence make this system a chemosensor for practical applications.[13] This phenomenon can be explained by the displacement of the coordinated zinc from the **SPHN** ligand by the strong ability of PPi to interact with **Receptor 1**. In mass spectrometry, the peak at m/z = 532.1211 [corresponding to **Receptor 1** + PPi + H^+ ≈ $C_{31}H_{25}N_5O_4$ + H^+]$^+$ (Fig. S22†) indicates the PPi induced displacement of zinc to **Receptor 1**. As shown in Scheme 2 the two zinc ions, each of them, possibly bind using four co-ordination to the cavity created by **SPHN** (which is also shown by Jobs plot analysis and HRMS). When PPi binds with **Receptor 1**, the two oxygens of each P atom of PPi first bind to the complexed Zn by creating penta co-ordination inflicting the detachment of the pyridine nitrogen from the Zn^{2+} ion, possibly the first step to start diminishing the Zn^{2+} ion induced fluorescence in **Receptor 1**. From the fluorescence titration experiment, the detection limit of **SPHN** for Zn^{2+} ions is determined to be 4.6 μM and 6.3 μM for PPi towards **Receptor 1** using the equation DL = $K \times Sb1/S$, where K = 3 and Sb_1 is the standard deviation of the blank solution and S is the slope of the calibration curve[14] (Fig. S4†). From the time *vs.* fluorescence intensity plot (Fig. S25†) at a fixed wavelength of 450 mm the rate constant[15] for the chelation induced fluorescence enhancement of **SPHN** with Zn^{2+} is found to be 4.6 × 10^{-3} s^{-1}. The equilibrium competition constant[16] is 5 × 10^4 M^{-1} on the basis of the fluorescence titration data (Fig. S2b†) in CH_3CN–10 mM aqueous HEPES buffer (7/3, v/v, 25 °C) solution at pH 7.4. The data are fitted to a displacement model that provides an equilibrium competition constant (Fig. S3†).

Theoretical study

The density functional theory calculation has been performed using the Gaussian 03 (Revision B.04)[17] package with "Gauss View" for the visualization of the molecular orbitals. Becke's three parameter hybrid-exchange functional, the nonlocal correlation provided by the Lee, Yang, and Parr expression, and the Vosko, Wilk, and Nuair 1980 local correlation functional (III) (B3LYP)[18] were used in the calculation. The 6-311+G(d,p) basis set was used for optimization of **SPHN** and for single-point energy calculations in the gas phase. Lanl2dz basis sets were used for Zn^{2+} and for the rest of the atoms 6-31G*+ basis sets were used for the optimization of the zinc complex in **Receptor 1** and the pyrophosphate linked complex. Time-dependent DFT (TD-DFT) calculations were also carried out using the 6-311+G(d,p) basis set in the gas phase for **SPHN**

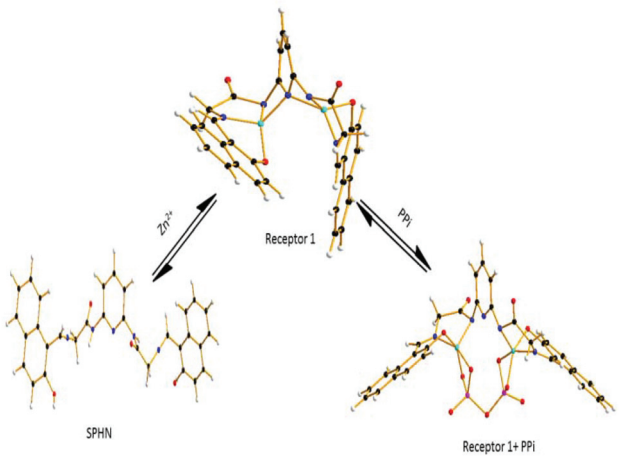

Scheme 2 Energy optimized structures of **SPHN**, (**SPHN** +Zn) **Receptor 1** and (**Receptor 1** + PPi).

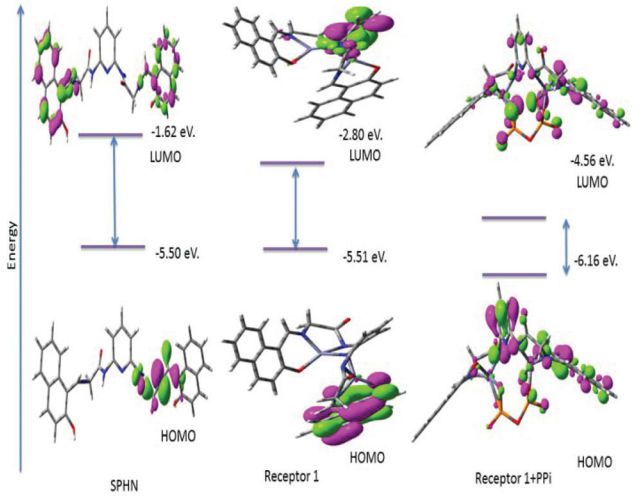

Fig. 7 HOMO and LUMO of **SPHN** and **Receptor 1** with an ISO value cut off 0.04.

(singlet excited states were calculated based on the singlet ground state geometry).

Time-dependent DFT (TD-DFT) calculation for the **SPHN–Zn** complex was performed using the same basis set as used in the optimization in the gas phase (singlet excited states were calculated based on the singlet ground state geometry). The DFT calculations show that in **SPHN** the donor sites are in *trans* orientation and on the addition of Zn^{2+} ions these donor sites of **SPHN** approach closer to each other and the complex experienced enough strain due to the coordination with zinc. Overall the complex molecule does not achieve extra stability as shown by the relative position of its HOMO over the HOMO of the free ligand (Fig. 7). Furthermore the HOMO–LUMO gap is also reduced. However on the addition of pyrophosphate the strain in **Receptor 1** is somewhat released as observed in the optimized structure of pyrophosphate linked to **Receptor 1** by which the coordination of the donor nitrogen atoms of **SPHN** is relieved and the coordination of the zinc ion is enhanced by the use of oxygen atoms from the pyrophosphate. This provides relative stability but the HOMO–LUMO gap in this system is drastically reduced. We have used only gas phase calculation but in reality the entire process occurs in solution and the relevant solvent correction would be more realistic to predict the relative stability of these three systems. However the addition of zinc ions and PPi to display fluorescence and its quenching alternately for several cycles confirm that the {**Receptor1** + $\mathbf{PP_i}$} complex ultimately releases PPi as a zinc salt releasing a free **SPHN** ligand for subsequent complex formation with the zinc ion followed by its scavenging using PPi. Due to this **Receptor 1** acts as a selective and sensitive pyrophosphate sensor. The electronic spectral absorptions of **SPHN** at 333, 350 and 438 nm are found to be close to the experimental absorptions observed at 300, 399 and 420 nm respectively. For **Receptor 1** theoretically calculated electronic spectral absorptions at 417 and 456 nm are close to the corresponding experimental electronic absorption peaks which appear at 400 and 420 nm respectively. This closeness in the photophysical properties in the experimental and theoretical results supports the nature of binding in **SPHN–Zn**.

Logic gate

The enhancement of fluorescence by zinc ions and the quenching of the fluorescence by PPi can be usefully employed in the construction of a logic gate. From the competition experiment, we observe that the enhancement of fluorescence by Zn^{2+} on coordination with **SPHN** has been quenched by the addition of PPi. To evaluate the exact phenomenon the reversibility test has been performed in which Zn^{2+} ions and PPi were added to **SPHN** in an alternate and reversible fashion (Fig. S6†). In the presence of Zn^{2+} ions the fluorescence of **SPHN** is enhanced, and on the addition of PPi to the solution of **Receptor 1** (**SPHN–Zn**) the enhanced fluorescence gradually decreases and again on further addition of Zn^{2+} to the mixture the fluorescence intensity once again increases. This type of reversible behaviour is like mimicking the **INHIBIT** logic gate (integrated[19] by combining a NOT, a YES and an AND gate {ESI}) at λ_{max} = 450 nm. A basic two-input **INHIBIT** can be obtained for **SPHN** ($c = 2 \times 10^{-5}$ M) with the action of Zn^{2+} ($c = 2 \times 10^{-4}$ M) and PPi anions ($c = 2 \times 10^{-4}$ M) as inputs. For the input, the fluorescence emission enhancement at 450 nm of **SPHN** in the presence of Zn^{2+} and in the absence of PPi is defined as the "1" state and in the other circumstances the quenching of the fluorescence of **SPHN** is defined as the "0" state. Zn^{2+} in this case should lead to fluorescence enhancement in its occupied state (at 450 nm) in the absence of PPi, equivalent to a YES operation (input 1).

The interaction of the other input, *i.e.* PPi in this case (input 2), with its corresponding receptor should lead to fluorescence quenching, thereby implementing the necessary **NOT** gate. The receptor, *i.e.* **SPHN** (occupied or free), acts in parallel on the fluorescence output signal, which implements the required **AND** function. In the presence of both inputs, the quenching (by input 2) should override the fluorescence enhancement by input 1, in accordance with the truth table and the circuit for the **INHIBIT** gate as shown in Fig. 8.

(a)

Input		Output
Zn^{2+}	PPi	INH(Fl.)
0	0	0
1	0	1
0	1	0
1	1	0

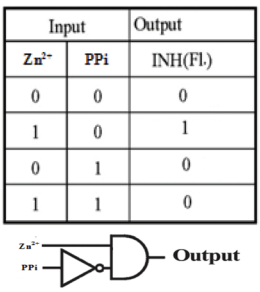

(b)

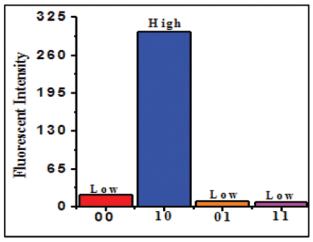

Fig. 8 (a) The logic table of the **INHIBIT** gate with the circuit. (b) Fluorescence output of **SPHN** ($c = 2 \times 10^{-5}$ M) at 450 nm (λ_{ex} = 400 nm) in the presence of chemical inputs, Zn^{2+} ($c = 2 \times 10^{-4}$ M) and PPi ($c = 2 \times 10^{-4}$ M) in CH_3CN–10 mM aqueous HEPES buffer (7/3, v/v, 25 °C) at pH = 7.4.

Cell imaging

For the bio-activity of **Receptor 1**, the membrane permeability of **SPHN** and its ability to specifically detect Zn^{2+} in living cells have been analysed. For this work HeLa cells were first incubated with Zn^{2+} ions followed by the addition of **SPHN** in one plate and **SPHN** and PPi together in another plate. A control incubation of the cells with the **SPHN** only was also carried out.

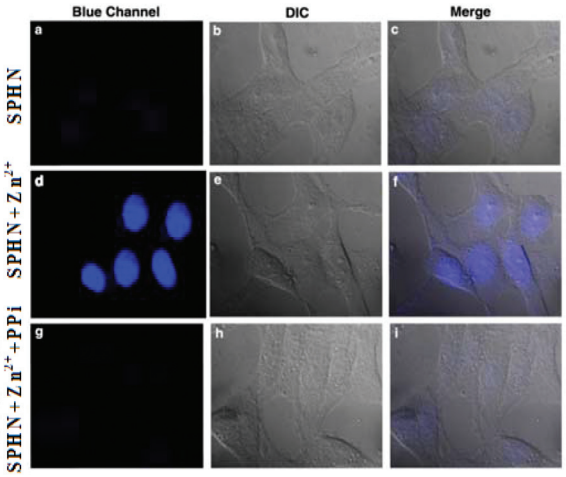

Fig. 9 HeLa cells showed intense blue fluorescence in the presence of both 50 μM each of **SPHN** and Zn^{2+} (d) and did not show any fluorescence in the absence of Zn^{2+} (a) and in the presence of PPi (g). Corresponding differential interference contrast (DIC) images (e, b and h) and merge images (f, c and i) of the cells are shown.

As shown in Fig. 9, the nuclei showed intense blue fluorescence in the blue channel when they were treated with Zn^{2+} followed by the receptor **SPHN** and the intensity was dramatically reduced upon treatment with PPi. The differential interference contrast showed very faint blue fluorescence when the cells were not treated with Zn^{2+}. The result clearly established that the receptor **SPHN** not only permeates the plasma membrane of the cells but also produces specific fluorescence in the nuclei in the presence of Zn^{2+} ions. Moreover the specific blue fluorescence was quenched in the presence of PPi. Thus, the receptor **SPHN** might act as a good nucleus marker in the presence of Zn^{2+} ions and the appearance of the blue color in the specific zone (nucleus) of the cell helps us to use it like a nuclear staining compound such as DAPI.

Conclusion

A new hydroxynaphthyl pyridine-Zn^{2+} complex (**Receptor 1**) bearing two Zn^{2+} centers has been investigated as a selective fluorescent chemosensor for PPi over other interfering anions in aqueous medium. Large fluorescence enhancement (blue fluorescence, 10 fold) by the addition of Zn^{2+} to the solution of **SPHN** and the quenching of this fluorescence upon addition of PPi were observed. The metal-anion induced 'Off–On–Off' type fluorescence response as a sensor has been carefully employed to function as a molecular switch. The binding phenomenon in the cascade pathway has been successfully established by the DFT method of calculation. The deep blue colored appearance of **SPHN** on zinc binding to the nucleus is successfully applied for use as a nucleus marker.

Experimental section

General

Unless otherwise mentioned, chemicals and solvents were purchased from Sigma-Aldrich chemicals Private Limited and were used without further purification. Melting points were determined on hot-plate melting point apparatus in an open-mouth capillary and are uncorrected. ^{1}H-NMR and ^{13}C-NMR spectra were recorded on a Brucker 300 MHz instrument. For NMR spectra, $CDCl_3$ and DMSO-d_6 were used as the solvent using TMS as an internal standard. Chemical shifts are expressed in δ units and ^{1}H–^{1}H and ^{1}H–C coupling constants are expressed in Hz. UV-vis titration experiments were performed on a JASCO UV-V530 spectrophotometer and the fluorescence experiment was performed using a PerkinElmer LS 55 fluorescence spectrophotometer and a fluorescence cell of 10 mm pathlength. IR spectra were recorded on a JASCO FT/IR-460 plus spectrometer, using KBr discs. The pH titration was carried out using an Agilent 8453 pH meter.

General method of UV-vis and fluorescence titrations

UV-vis method. For UV-vis titrations of cations, a stock solution of **SPHN** was prepared in CH_3CN–aqueous HEPES buffer (7/3, v/v, 25 °C) at pH 7.4. The solution of the guest cation, the zinc ion, using its chloride salt of the order of 2×10^{-4} M was also prepared in CH_3CN–10 mM aqueous HEPES buffer (7/3, v/v, 25 °C) at pH = 7.4. Solutions of various concentrations of the sensor and various concentrations of cations were prepared separately. The spectra of these solutions were recorded by means of UV-vis spectroscopy.

Fluorescence method. For fluorescence titrations, a stock solution of **SPHN** and **Receptor 1** was prepared at 20 μM concentration in CH_3CN–10 mM aqueous HEPES buffer (7/3, v/v, 25 °C) at pH 7.4. The solutions of the guest cations like Co^{2+}, Hg^{2+}, Mn^{2+}, Ni^{2+}, Pb^{2+}, Cd^{2+}, Zn^{2+}, Mg^{2+}, Cu^{2+}, Fe^{3+}, Cr^{3+}, Ca^{2+}, Mg^{2+}, Na^+ and K^+ as their chloride salts of the order of 200 μM were also prepared in deionized water. The solutions of the guest anions using various anions like F^-, AcO^-, Cl^-, Br^-, I^-, $C_6H_5COO^-$, ATP, DHP, NO_3^-, NO_2^-, SO_3^{2-}, HPO_4^{2-}, and $P_2O_7^{4-}$ as their tetrabutyl ammonium salts of the order of $c = 2 \times 10^{-4}$ M were also prepared. Solutions of various concentrations of a sensor and increasing concentrations of cations and anions were prepared separately. The fluorescence spectra of these solutions were then recorded as described in the text.

Determination of the fluorescence quantum yield

Here, the quantum yield φ was measured using the following equation:

$$\varphi_x = \varphi_s\ (F_x/F_s)(A_s/A_x)(n_x^2/n_s^2)$$

where X and S indicate the unknown and standard solution respectively, φ = quantum yield, F = area under the emission curve, A = absorbance at the excitation wavelength, and n = index of refraction of the solvent. Here φ measurements were performed using anthracene in ethanol as a standard [φ = 0.27] (error ~ 10%).

Cell culture and fluorescence microscopy

In order to perform fluorescence microscopy, HeLa cells were grown in Dulbecco's modified Eagle's medium (DMEM) supplemented with 10% fetal bovine serum and penicillin–streptomycin solution (0.5 U ml^{-1} of penicillin and 0.5 μg ml^{-1} of streptomycin) on cover slips in 35 mm dishes at 37 °C in an atmosphere of air with 5% CO_2 and constant humidity. Initially, the cells were incubated with 50 μM of Zn^{2+} in the growth medium for an hour. Then the cells were washed with phosphate buffered saline (PBS) followed by the addition of a fresh growth medium containing 50 μM of the receptor **SPHN** and for other fraction of the cells with both the receptor **SPHN** and inhibitor PPi. The cells were further incubated for 45 minutes. Following incubation the cells were washed three times with PBS and cross-linked with 4% HCHO. Finally, the cover slip was mounted on a glass slide and the imaging was carried out using a Zeiss Axio Observer Fluorescence Microscope with an Apotome attachment.

Synthetic steps for preparation of SPHN and the SPHN–Zn complex (Receptor 1)

Synthesis of 2-hydroxy-1-napthylaldehyde. 2-Hydroxy-1-napthylaldehyde was synthesized by the reported procedure.[20] β-Naphthol (1 g, 0.0069 mol) was placed in a 100 ml r.b. flask fitted with a reflux condenser, a magnetic stirrer and a dropping funnel. It was then dissolved in EtOH at 80–90 °C. NaOH (2 g, 0.05 mol) in 20 ml water was then added dropwise to this hot solution and the solution became darker. After half an hour, $CHCl_3$ (1.3 g, 0.011 mol) was added dropwise using a dropping funnel. Development of deep blue coloration indicates that the reaction has started. Near the end point of the addition, the sodium salt of the phenolic aldehyde separated out. The reaction mixture was stirred for six hours. Excess ethanol and chloroform were distilled off. The dark oil left was mixed with a considerable amount of sodium chloride. Sufficient water was added to dissolve the salt, and the oil was separated and washed with hot water. Then, the solution was neutralized with dilute hydrochloric acid and extracted with chloroform. Finally, the product was purified by 60–120 silica gel with 1–2% ethyl acetate in pet ether. The yield of the product was 500 mg (50%). Melting point: 79–80 °C.

Synthesis of compound A. 2,6-Diaminopyridine (1 g, 9.09 mmol) was dissolved in dry dichloromethane at 0–5 °C in an ice bath and triethylamine (5 ml) was added to the reaction mixture. Chloroacetyl chloride (8 ml) was added to this reaction mixture dropwise using a dropping funnel. White precipitate of triethylamine salt separated out immediately. The reaction mixture was stirred at room temperature under a nitrogen atmosphere for 3 h. After completion of the reaction, water was added to the reaction mixture and the organic layer was separated out and dried under high vacuum. The final product was purified by column chromatography using 6–8% ethyl acetate in pet ether to give a white solid.

Yield −1.5 g; 62%. Mp 130–140 °C. **^{1}H NMR ($CDCl_3$, 300 MHz): δ (ppm):** 8.41 (s, 1H), 7.95 (d, 1H, J = 8.01 Hz), 7.75 (t, 1H, J = 9 Hz), 4.16 (s, 2H). **^{13}C NMR ($CDCl_3$, 75 MHz): δ (ppm):** 165.00, 145.95, 140.77, 108.08, 65.40. HR**MS (ESI-TOF) *m*/*z*:** M+ calculated for $C_9H_9Cl_2N_3O_2$ is 261.0072; found: 262.0070 $(M + H)^+$.

Synthesis of compound B. Compound **A** (1 g, 3.83 mmol) was stirred at 60–80 °C in dry DMF (20 ml) for half an hour. After half an hour sodium azide (800 mg) was added to it and the reaction mixture was stirred for 6 h at 60–80 °C. After completion of the reaction, the reaction mixture was added to water and a white precipitate separated out. The precipitate was filtered and dissolved in chloroform and purified by column chromatography using 20–30% ethyl acetate in pet ether to afford compound **B**.

Yield – 800 mg, 75%. **Mp** – 165–170 °C. **^{1}H NMR (DMSO-d_6, 300 MHz): δ (ppm):** 8.41 (s, 1H), 7.94 (d, 1H, J = 7.95 Hz), 7.75 (t, 1H, J = 8.05 Hz), 4.29 (s, 2H). **^{13}C NMR (DMSO-d_6, 75 MHz): δ (ppm):** 177.00, 165.77, 140.95, 110.08, 65.77. HR**MS (ESI-TOF) *m*/*z*:** M+ calculated for $C_9H_9N_9O_2$ is 275.0879; found: 276.0876 $(M + H)^+$.

Synthesis of compound C. Compound **B** (700, 2.55 mmol) was taken in a 100 ml r.b. flask which was then placed under high vacuum using a two neck stopper. The compound was dissolved in dry methanol and H_2 – Pd/C (200 mg) was added to the reaction mixture. For every half an hour the r.b. flask is placed under vacuum to remove moisture. After completion of the reaction, the reaction mixture was passed through a celite bed and the bed was washed with 5% chloroform in methanol. Finally the solvent was evaporated to dryness and the product was purified by crystallization using 2–3% chloroform in methanol to produce a white amine, compound **C**.

Yield – 400 mg, 70%. Mp – 180–190 °C. **^{1}H NMR ($CDCl_3$, 300 MHz): δ (ppm):** 8.41 (s, 1H), 7.94 (d, 1H, J = 7.95 Hz), 7.75 (t, 1H, J = 8.05 Hz), 4.16 (s, 2H), 2.20 (s, 2H). **^{13}C NMR ($CDCl_3$, 75 MHz): δ (ppm):** 170.08, 145.33, 140.82, 108.08, 40.65. **HRMS (ESI-TOF) *m*/*z*:** M+ calculated for $C_9H_{13}N_5O_2$ is 223.1069; found: 224.1060 $(M + H)^+$.

Synthesis of the receptor SPHN. The amine **C** (300 mg, 1.751 mmol) and 2-hydroxy-1-naphthaldehyde (300 mg, 1.744 mmol) were taken together and stirred in dry methanol (20 mL) at room temperature for 4 h. A greenish white precipitate separated out which was filtered out and washed with methanol. The greenish white solid product was recrystallized in absolute ethanol to provide the white solid compound, **SPHN**.

Yield: 400 mg, 77%, **Mp:** 200–210 °C. **FT-IR (KBr, cm^{-1}):** 1107, 1244, 1468, 1501, 1619, 1691, 2333, 2359, 2850, 2922, 3170, 3323(broad, –OH). **^{1}H NMR (DMSO-d_6, 300 MHz):** δ (ppm): 13.75 (d, 1H, J = 5.07 Hz), 10.45 (s, 1H), 9.06 (d, 1H, J = 10.17 Hz), 8.02 (d, 1H, J = 8.31 Hz), 7.75 (m, 2H), 7.62 (d, 1H, J = 7.89 Hz), 7.42 (t, 1H, J = 14.4 Hz), 7.19 (t, 1H, J = 14.07 Hz), 6.72 (d, 1H, J = 9.33 Hz), 4.63 (s, 2H). **^{13}C NMR (DMSO-d_6, 75 MHz): δ (ppm):** 164.63, 158.30, 154.67, 140.26, 136.67, 136.22, 132.09, 129.67, 128.22, 127.25, 127.07, 123.95, 119.21, 112.78, 108.94, 55.29. HR**MS (ESI-TOF) *m*/*z*:** M+ calculated for $C_{31}H_{25}N_5O_4$ is 531.1907; found: 532.1094 $(M + H)^+$. **Elemental analysis:** calculated value: C, 70.04; H, 4.74; N, 13.18. Observed value: C, 70.16; H, 4.67; N, 13.13%.

Synthesis of the SPHN–Zn complex (Receptor 1). The Zn^{2+} complex of the SPHN was synthesized by adding the SPHN (300 mg, 0.808 mmol) to a methanol solution of $ZnCl_2$ (303 mg, 0.807 mmol) and the whole mixture was stirred for 30 minutes. The solvent was removed under vacuum and recrystallized by dissolving in dry ethanol and the whole mass was washed with diethyl ether several times. Finally a greenish white solid was obtained (200 mg, 60%) and characterized by mass spectrometry (ESI-TOF) and IR analysis (ESI†).

FT-IR (KBr, cm^{-1}): 1155, 1263, 1468, 1501, 1619, 1691, 2333, 2359, 2850, 2900, 3170. **HRMS (ESI-TOF) *m*/*z*:** M+ calculated for $C_{31}H_{21}N_5O_4Zn_2$ is 655.0176; found: 656.0172. **Elemental analysis:** calculated value: C, 56.56; H, 3.22; N, 10.64. Observed value: C, 56.52; H, 3.24; N, 10.66%.

Acknowledgements

The authors thank the DST and CSIR (Govt of India) for financial support. A.K.D., B.P., S.R. and A.K.M. acknowledge the CSIR for providing fellowships.

Notes and references

1 (*a*) N. Shao, H. Wang, X. Gao, R. Yang and W. Chan, *Anal. Chem.*, 2010, **82**, 4628; (*b*) Y. Kurishita, T. Kohira, A. Ojida and I. Hamachi, *J. Am. Chem. Soc.*, 2010, **132**, 13290; (*c*) P. Mahato, A. Ghosh, A. Shrivastav, S. K. Mishra, S. Mishra and A. Das, *Chem. Commun.*, 2010, **46**, 9134.

2 (*a*) Q. Li, S. J. Lee, C. Ha, C. B. Park, G. Yang, W. B. Gan and Y. T. Chang, *Angew. Chem., Int. Ed.*, 2004, **43**, 6331; (*b*) J. Gao, S. Watanabe and E. T. Kool, *J. Am. Chem. Soc.*, 2004, **126**, 12748; (*c*) H. W. Rhee, H. Y. Choi, K. Han and J. I. Hong, *J. Am. Chem. Soc.*, 2007, **129**, 4524.

3 (*a*) B. A. Smith, W. J. Akers, W. M. Leevy, A. J. Lampkins, S. Xiao, W. Wolter, M. A. Suckow, S. Achilefu and B. D. Smith, *J. Am. Chem. Soc.*, 2010, **132**, 67; (*b*) W. M. Leevy, S. Gammon, T. H. Jiang, J. R. Johnson, D. J. Maxwell, E. N. Jackson, M. Marquez, D. P. Worms and B. D. Smith, *J. Am. Chem. Soc.*, 2006, **128**, 16476.

4 (*a*) R. Martínez-Manez and F. Sancenon, *Chem. Rev.*, 2003, **103**, 4419; (*b*) Z. Xu, S. K. Kim and J. Yoon, *Chem. Soc. Rev.*, 2010, **39**, 1457; (*c*) P. A. Gale, *Chem. Soc. Rev.*, 2010, **39**, 3746; (*d*) S. K. Kim and J. L. Sessler, *Chem. Soc. Rev.*, 2010, **39**, 3784; (*e*) A. F. Li, J. H. Wang, F. Wang and Y. B. Jiang, *Chem. Soc. Rev.*, 2010, **39**, 3729; (*f*) H. N. Lee, K. M. K. Swamy, S. K. Kim, J. Y. Kwon, Y. Kim, S. J. Kim, Y. J. Yoon and J. Yoon, *Org. Lett.*, 2007, **9**, 243; (*g*) Y. Xie, P. Wei, X. Li, T. Hong, K. Zhang and H. Furuta, *J. Am. Chem. Soc.*, 2013, **135**, 19119; (*h*) Y. Ding, X. Li, T. Li, W. Zhu and Y. Xie, *J. Org. Chem.*, 2013, **78**, 5328.

5 (*a*) W. N. Lipscomb and N. Strater, *Chem. Rev.*, 1996, **96**, 2375; (*b*) M. Ronaghi, S. Karamohamed, B. Pettersson, M. Uhlen and P. Nyren, *Anal. Biochem.*, 1996, **242**, 84; (*c*) T. Tabary and L. Ju, *J. Immunol. Methods*, 1992, **156**, 55; (*d*) S. K. Kim, D. H. Lee, J. I. Hong and J. Yoon, *Acc. Chem. Res.*, 2009, **42**, 23.

6 (*a*) Y. Zhou, Z. Xu and J. Yoon, *Chem. Soc. Rev.*, 2011, **40**, 2222; (*b*) T. H. Kwon, H. J. Kim and J. I. Hong, *Chem. – Eur. J.*, 2008, **14**, 9613; (*c*) Y. Kurishita, T. Kohira, A. Ojida and I. Hamachi, *J. Am. Chem. Soc.*, 2010, **132**, 13290.

7 (*a*) J. H. Lee, A. R. Jeong, J. H. Jung, C. M. Park and J. I. Hong, *J. Org. Chem.*, 2011, **76**, 417; (*b*) X. Zhao and K. S. Schanze, *Chem. Commun.*, 2010, **46**, 6075; (*c*) S. Xu, M. He, H. Yu, X. Cai, X. Tan, B. Lu and B. Shu, *Anal. Biochem.*, 2001, **299**, 188.

8 (*a*) M. Doherty, C. Becher, M. Regan, A. Jones and J. Ledingham, *Ann. Rheum. Dis.*, 1996, **55**, 432.

9 (*a*) S. Mizukami, T. Nagano, Y. Urano, A. Odani and K. Kikuchi, *J. Am. Chem. Soc.*, 2002, **124**, 3920; (*b*) A. Ojida, H. Nonaka, Y. Miyahara, S. Tamaru, K. Sada and I. Hamachi, *Angew. Chem., Int. Ed.*, 2006, **45**, 5518.

10 (*a*) M. J. Kim, K. M. K. Swamy, K. M. Lee, A. R. Jagdale, Y. Kim, S. J. Kim, K. H. Yoo and J. Yoon, *Chem. Commun.*, 2009, 7215; (*b*) D. H. Lee, S. Y. Kim and J. I. Hong, *Angew. Chem., Int. Ed.*, 2004, **43**, 4777; (*c*) H. N. Lee, Z. Xu, S. K. Kim, K. M. Swamy, Y. Kim, S. J. Kim and J. Yoon, *J. Am. Chem. Soc.*, 2007, **129**, 3828; (*d*) S. K. Kim, D. G. Lee, J. I. Hong and J. Yoon, *Acc. Chem. Res.*, 2009, **42**, 23; (*e*) X. Zhaoa and C. Zhi Huang, *Analyst*, 2010, **135**, 2853; (*f*) G. Ambrosi, M. Formica, V. Fusi, L. Giorgi, A. Guerri, E. Macedi, M. Micheloni, P. Paoli, R. Pontellini and P. Rossi, *Inorg. Chem.*, 2009, **48**, 5901.

11 (*a*) A. J. Benesi and H. Hildebrand, *J. Am. Chem. Soc.*, 1949, **71**, 2703; (*b*) Y. Shiraishi, S. Sumiya, Y. Kohno and T. Hirai, *J. Org. Chem.*, 2008, **73**, 8571.

12 (*a*) S. Goswami, A. K. Das, K. Aich, A. Manna, S. Maity, K. Khanra and N. Bhattacharyya, *Analyst*, 2013, **138**, 4593–4598; (*b*) S. Goswami, A. Manna, S. Paul, K. Aich, A. K. Das and S. Chakraborty, *Dalton Trans.*, 2013, **42**, 8078; (*c*) S. Goswami, A. K. Das and S. Maity, *Dalton Trans.*, 2013, **42**, 16259; (*d*) S. Goswami, A. K. Das, A. K. Maity, A. Manna, K. Aich, S. Maity, P. Saha and T. K. Mandal, *Dalton Trans.*, 2014, **43**, 231; (*e*) S. Goswami, A. K. Das, D. Sen, K. Aich, H.-K. Fun and C. K. Quah, *Tetrahedron Lett.*, 2012, **53**, 4819; (*f*) S. Goswami, A. K. Das, K. Aich and A. Manna, *Tetrahedron Lett.*, 2013, **54**, 4215; (*g*) S. Goswami, A. K. Das,

K. Aich, A. Manna, H.-K. Fun and C. K. Quah, *Supramol. Chem.*, 2014, **26**, 94.

13 E. M. Nolan, M. E. Racine and S. J. Lippard, *Inorg. Chem.*, 2006, **45**, 2742–2749.

14 (*a*) M. Shortreed, R. Kopelman, M. Kuhn and B. Hoyland, *Anal. Chem.*, 1996, **68**, 1414; (*b*) W. Lin, L. Yuan, Z. Cao, Y. Feng and L. Long, *Chem. – Eur. J.*, 2009, **15**, 5096; (*c*) M. Zhu, M. Yuan, X. Liu, J. Xu, J. Lv, C. Huang, H. Liu, Y. Li, S. Wang and D. Zhu, *Org. Lett.*, 2008, **10**, 1481.

15 B. Chen, Y. Ding, X. Li, W. Zhu, J. P. Hill, K. Arigac and Y. Xie, *Chem. Commun.*, 2013, **49**, 10136.

16 (*a*) C. R. Lohani, J. M. Kim, S. Y. Chung, J. Yoon and K. H. Lee, *Analyst*, 2010, **135**, 2079; (*b*) A. R. Reddi, T. R. Guzman, R. M. Breece, D. L. Tiemey and B. R. Gibney, *J. Am. Chem. Soc.*, 2007, **129**, 12815.

17 M. J. Frisch, G. W. Trucks, H. B. Schlegel, G. E. Scuseria, M. A. Robb, J. R. Cheeseman, J. A. Montgomery Jr., T. Vreven, K. N. Kudin, J. C. Burant, J. M. Millam, S. S. Iyengar, J. Tomasi, V. Barone, B. Mennucci, M. Cossi, G. Scalmani, N. Rega, G. A. Petersson, H. Nakatsuji, M. Hada, M. Ehara, K. Toyota, R. Fukuda, J. Hasegawa, M. Ishida, T. Nakajima, Y. Honda, O. Kitao, H. Nakai, M. Klene, X. Li, J. E. Knox, H. P. Hratchian, J. B. Cross, V. Bakken, C. Adamo, J. Jaramillo, R. Gomperts, R. E. Stratmann, O. Yazyev, A. J. Austin, R. Cammi, C. Pomelli, J. W. Ochterski, P. Y. Ayala, K. Morokuma, G. A. Voth, P. Salvador, J. J. Dannenberg, V. G. Zakrzewski, S. Dapprich, A. D. Daniels, M. C. Strain, O. Farkas, D. K. Malick, A. D. Rabuck, K. Raghavachari, J. B. Foresman, J. V. Ortiz, Q. Cui, A. G. Baboul, S. Clifford, J. Cioslowski, B. B. Stefanov, G. Liu, A. Liashenko, P. Piskorz, I. Komaromi, R. L. Martin, D. J. Fox, T. Keith, M. A. Al-Laham, C. Y. Peng, A. Nanayakkara, M. Challacombe, P. M. W. Gill, B. Johnson, W. Chen, M. W. Wong, C. Gonzalez and J. A. Pople, *Gaussian 03 (Revision B.04)*, Gaussian, Inc., Pittsburgh, PA, 2003.

18 (*a*) A. D. Becke, *J. Chem. Phys.*, 1993, **98**, 5648; (*b*) C. Lee, W. Yang and R. G. Parr, *Phys. Rev. B: Condens. Matter*, 1988, **37**, 785.

19 A. P. de Silva, I. M. H. Dixon, Q. N. Gunaratne, T. Gunnlaugsson, P. R. S. Maxwell and T. E. Rice, *J. Am. Chem. Soc.*, 1999, **121**, 1393.

20 (*a*) Fosse, *Bull. Soc. Chim. Fr.*, 1901, **25**, 373; (*b*) Kolesnikov, Korshak and Krakovnaya, *Zh. Obshch. Khim.*, 1951, **21**, 397, (*Chem. Abstr.*, 1951, **45**, 7553).